

**Issues in the Analysis and Testing of Textile Composites  
with Large Representative Volume Elements**

by

**Gerd Weissenbach**

ISBN: 1-58112-245-4

**DISSERTATION.COM**



Boca Raton, Florida  
USA • 2004

*Issues in the Analysis and Testing of Textile Composites  
with Large Representative Volume Elements*

Copyright © 2003 Gerd Weissenbach  
All rights reserved.

Dissertation.com  
Boca Raton, Florida  
USA • 2004

ISBN: 1-58112-245-4

Issues in the analysis and testing of textile composites with  
large representative volume elements

Gerd Weissenbach

Diplom-Ingenieur (FH)

Faculty of Engineering and Built Environment of the University of Ulster

Thesis submitted for the degree of Doctor of Philosophy

March 2003

## Contents

<b>Acknowledgements</b> .....	5
<b>Summary</b> .....	6
<b>Abbreviations</b> .....	7
<b>Note on access to contents</b> .....	9
<b>List of figures</b> .....	10
<b>List of tables</b> .....	12
<b>1 Introduction</b> .....	13
1.1 Textile composite materials .....	13
1.2 Application of textile composite materials .....	16
1.2.1 Composite component of a lower leg prosthesis .....	16
1.2.2 T-sections .....	21
1.2.3 Implications .....	27
<b>2 Aims and objectives</b> .....	29
<b>3 Literature review</b> .....	31
3.1 Analysis .....	31
3.1.1 Global/local analysis .....	32
3.1.2 Macro elements .....	33
3.1.3 Mesovolumes .....	34
3.1.4 Conclusion .....	36
3.2 Shear testing .....	37
<b>4 Rationale</b> .....	44
4.1 Structural analysis of textile composites .....	44
4.2 Functional description of the material stiffness .....	47
4.3 Stiffness function .....	53
4.3.1 Akima sub-spline interpolation .....	53
4.3.2 Examples of stiffness functions .....	59
4.4 Finite element approach .....	61
4.4.1 Average material stiffness .....	62
4.4.2 Stiffness at integration points .....	66

<b>5 Results and discussion</b> .....	67
5.1 Application to material tests.....	67
5.1.1 Plate twist test.....	68
5.1.2 V-notched beam shear test.....	74
5.1.3 Conclusions for general cases.....	86
5.2 Comparison of the different finite element approaches.....	91
5.3 Electronic speckle pattern interferometry.....	94
<b>6 Conclusions</b> .....	101
<b>7 Further work</b> .....	104
7.1 Three-dimensional problems.....	104
7.2 Plate bending.....	105
7.3 Failure criteria.....	108
<b>8 References</b> .....	110
<b>Appendices</b> .....	A1
A1 Publications.....	A2
A2 Finite element analysis.....	A4
A2.1 Principles.....	A4
A2.2 Isoparametric quadrilateral finite elements.....	A9
A2.3 Material laws.....	A13
A2.4 Gauss integration.....	A18
A3 Program description.....	A23
A3.1 General.....	A23
A3.2 Structure of input file.....	A27
A4 Software tests.....	A31
A4.1 Tensile test.....	A31
A4.2 Biaxial test.....	A35
A4.3 Beam bending.....	A37
A4.4 Bimetallic beam.....	A42
A5 Program listings.....	A47
A5.1 STATEC (main program).....	A49

A5.2	READDAT .....	A56
A5.3	ASSEMK .....	A64
A5.4	QUAD .....	A69
A5.5	CHOM .....	A77
A5.6	CAVRG .....	A80
A5.7	CHET .....	A88
A5.8	STFFNK2D .....	A92
A5.9	MAPP2D .....	A96
A5.10	SPL2D .....	A99
A5.11	SPL1D .....	A102
A5.12	DMACH .....	A108
A5.13	BMATR .....	A109
A5.14	ASSEMF .....	A113
A5.15	REDUC .....	A116
A5.16	SOLVE .....	A119
A5.17	GAUSS .....	A122
A5.18	GAUSSP .....	A124
A5.19	GAUSSS .....	A127
A5.20	MACHPD .....	A129
A5.21	STRAIN .....	A130
A5.22	STRESS .....	A136
A5.23	WRITEGID .....	A142
A6	Software tools .....	A148
A6.1	RVESCALE .....	A149
A6.2	RANDOMISE .....	A155
A6.3	SHEAR .....	A160

## **Acknowledgements**

This work could not have been written without the help and support of the following people.

First and foremost I would like to thank my supervisors Dr. Desmond Brown and Prof. Robert McIlhagger for their unceasing support and encouragement.

I am very grateful to my wife Chao-Ling for her strong support and encouragement. Without her help this thesis would not have been possible. I also would like to thank my parents Karlheinz and Josefine Weißenbach for their help in getting me started.

I also would like to thank the following people who made a direct or indirect contribution to the completion of this work (in alphabetic order): Roy Brelsford, Roy Carton, Jim Curran, Dr. Michael Harris, Prof. Dr.-Ing. Franz Josef Lange, Ludwig Limmer, Stewart Matthews, Konrad and Irene Mayr, Dr. Julie Soden and the other people at the Engineering Composites Research Centre.

Finally, I would like to thank all my friends who helped to enjoy life after work.

## Summary

The high degree of heterogeneity of textile composites was found to be the primary problem in analysis and testing. A concept was developed based on a description of the local variation of the material stiffness matrix using a spline interpolation. The role of this stiffness function is to facilitate the calculation of the material stiffness matrix at any given position or for arbitrary domains in the form of finite elements.

Based on this approach, two different methods were developed. In the first method the average material stiffness matrix is calculated for a finite element and subsequently the elemental stiffness matrix of this element is assembled. In the second approach the elemental stiffness matrix is calculated directly using the local material stiffness at the integration points of the finite element.

This concept was then applied to the plate twist test. The numerical analysis of this test was done in order to determine the influence of heterogeneity on the test results. It was shown that this test measures the in-plane shear modulus largely independent of the representative volume element (RVE) size.

Both finite element approaches were then applied to the V-notched beam shear test, to investigate the applicability of this test to the measurement of the shear properties. The test set-up as well as numerical parameters of the finite element analysis of the test were studied. It was possible to derive limits for the applicability of the V-notched beam shear test in terms of RVE size, as well as set up guidelines for the finite element analysis of textile composites.

With electronic speckle pattern interferometry, which enables full-field displacement and strain measurements, tensile tests were carried out on 3D-woven textile composite specimens. With the agreement of the experimental results and the theoretical predictions the validity of the developed approach was again shown.

## Abbreviations

isotropic	material properties independent of orientation
orthotropic	material properties as a function of orientation with three mutually perpendicular planes of symmetry
anisotropic	material properties in the general case; no planes of symmetry
homogeneous	constant material properties
heterogeneous	material properties as a function of position
micro-mechanics	area in mechanics about calculating the effective material properties from the properties of the constituent materials
macro-mechanics	mechanics of homogeneous materials
meso-mechanics	area in mechanics between micro-mechanics and macro-mechanics
homogenisation	process of determining the effective material properties of a heterogeneous material
RVE	<b>Representative Volume Element</b>
sub-volume	subdivision of a RVE (also often called sub-cell)
stiffness function	material stiffness matrix as a function of the spatial co-ordinates
ESPI	<b>Electronic Speckle Pattern Interferometry</b> (full field strain measurement method)
I-DEAS™	design and analysis software from SDRC®
XS	Cross-Sectional-Program (software developed at the Engineering Composites Research Centre for weave structure design)

ELCOTEC	<b>Elastic Constants of Textile Composites</b> (software developed at the Engineering Composites Research Centre for the prediction of elastic constants)
STATEC	<b>Structural Analysis of Textile Composites</b> (software developed at the Engineering Composites Research Centre for structural analysis)
GiD	finite element pre- and postprocessor (software developed at the International Center for Numerical Methods in Engineering in Barcelona)

Symbols:

(Matrices and vectors are printed in **bold** letters; scalars in *italic* letters)

<b>C</b>	material stiffness matrix
<b>D</b>	differential operator
<b>N</b>	shape function
<b>B</b>	strain shape function
<b>k</b>	elemental stiffness matrix
<b>K</b>	global stiffness matrix of the finite element model
<b>f</b>	local nodal forces
<b>F</b>	global external nodal forces
<b>u</b>	displacements
<b><math>\epsilon</math></b>	strain vector
<b><math>\sigma</math></b>	stress vector
<i>E</i>	Elastic modulus
<i>G</i>	shear modulus
<i>v</i>	Poisson's ratio
$\xi, \eta$	local co-ordinates (“ksi” and “eta” respectively)

**Note on access to contents**

“I hereby declare that for one year following the date on which the thesis is deposited in the Library of the University of Ulster, the thesis shall remain confidential with access or copying prohibited. Following expiry of this period I permit the Librarian of the University to allow the thesis to be copied in whole or in part without reference to me on the understanding that such authority applies to the provision of single copies made for study purposes or for inclusion within the stock of another library. *This restriction does not apply to the British Library Thesis Service (which, subject to expiry of the period of confidentiality, is permitted to copy the thesis on demand for loan or sale under the terms of a separate agreement) nor to the copying or publication of the title and abstract of the thesis.* IT IS A CONDITION OF USE OF THIS THESIS THAT ANYONE WHO CONSULTS IT MUST RECOGNISE THAT THE COPYRIGHT RESTS WITH THE AUTHOR AND THAT NO QUOTATION FROM THE THESIS AND NO INFORMATION DERIVED FROM IT MAY BE PUBLISHED UNLESS THE SOURCE IS PROPERLY ACKNOWLEDGED.”

## List of figures

Figure 1: Integrally woven double-bladed T-skin and I-beam.....	14
Figure 2: Examples of complex 3D-weave structures (cross-sections).....	15
Figure 3: An athlete with similar lower leg prostheses .....	18
Figure 4: Lower leg prosthesis developed at the University of Ulster .....	19
Figure 5: Forces during stance phase.....	20
Figure 6: Test set-up for interplane testing .....	23
Figure 7: Schematic force-deflection curve .....	24
Figure 8: Microsections of cleavage area .....	24
Figure 9: Force/deflection curves with increasing interlinking .....	26
Figure 10: Test set-up for the short beam shear test.....	38
Figure 11: Test set-up for the three-rail shear test.....	39
Figure 12: Test set-up for the V-notched beam shear test .....	41
Figure 13: Test set-up for the plate twist test.....	42
Figure 14: Displacement fields of shear specimen using Moiré interferometry...	45
Figure 15: Finite element mesh superimposed on 8 harness satin weave .....	46
Figure 16: RVE and geometric features .....	46
Figure 17: Microsection of a typical 3D-woven textile composite .....	48
Figure 18: Solid model of RVE.....	48
Figure 19: Procedure to incorporate stiffness variation within RVE .....	52
Figure 20: Comparison of two interpolation methods.....	54
Figure 21: Continuity and periodicity between adjacent RVEs.....	55
Figure 22: Interpolation in two dimensions .....	59
Figure 23: Stiffness variations of a plain weave composite.....	60
Figure 24: Stiffness variations of a 3D-woven composite.....	61
Figure 25: Gauss grid with $10 \times 10$ sampling points.....	64
Figure 26: Reduction of discontinuities using mesh refinement.....	65
Figure 27: Error dependent on material orientation and orthotropy ratio.....	70
Figure 28: Correction factor $CF$ for $R/L = 0.95$ .....	71
Figure 29: Stiffness variation within composite material of chessboard pattern..	72
Figure 30: Displacement and strain fields .....	73

Figure 31: Plate deflection with varying number of RVEs.....	73
Figure 32: Mesh and boundary conditions of the V-notched beam shear test.....	75
Figure 33: Shear gauge measurement area .....	76
Figure 34: Detailed mesh view of measurement area.....	76
Figure 35: Correction factor for the V-notched beam shear test.....	78
Figure 36: RVE with circular inclusion.....	79
Figure 37: Sub-volume stiffness.....	80
Figure 38: RVE positions relative to measurement area .....	82
Figure 39: Shear strain of specimen with different RVE-sizes.....	84
Figure 40: Result of shear measurements with different RVE sizes .....	85
Figure 41: Envelope for the shear measurement variations.....	86
Figure 42: Finite element ratio for averaged material properties.....	89
Figure 43: Finite element ratio for heterogeneous material properties.....	90
Figure 44: Number of required integration points for different finite element ratios	90
Figure 45: Comparison of shear modulus for different approaches.....	92
Figure 46: Comparison of shear strain variations for different approaches.....	93
Figure 47: Mini-3D-ESPI-System for full-field strain measurements .....	94
Figure 48: Optical configuration of the ESPI system.....	95
Figure 49: Flowchart for solving 3D problems.....	97
Figure 50: Normal strain in loading direction.....	98
Figure 51: Experimental results and theoretical predictions.....	99
Figure 52: Effects of weave structure irregularity.....	100

**List of tables**

Table 1: Comparison of weights of parts with equal stiffness .....	22
Table 2: Predicted and experimental elastic stiffness data .....	51

# 1 Introduction

## *1.1 Textile composite materials*

In aerospace engineering unidirectionally reinforced laminated composite materials are very common for high performance parts requiring low weight. This kind of material is used because of its high strength-to-weight and high stiffness-to-weight ratio under membrane loading. Additionally, the in-plane performance of the material can be tailored to the applied stresses and capitalise on the anisotropic material behaviour. However, out-of-plane performance, such as during impact loading, is very weak, as these materials are designed for membrane loading, i.e. two-dimensional stress states and not for three-dimensional stresses. In the through-the-thickness direction a laminate is only held together by the matrix, which leads to low damage tolerance and the problem of delamination.

The low damage tolerance of laminated materials can lead to premature failure and limited fatigue life. The failure initiates in local damage caused by three-dimensional stresses, for example from impact. This local failure of the material can progress between two layers of the laminate because of the lack of any mechanism to prevent further delamination. In a worst case scenario this can lead to catastrophic failure of the composite component. For this reason, damage tolerance becomes the primary design variable for this kind of material, which greatly reduces the originally expected benefit of using a material with such high specific in-plane strength and stiffness.

The low damage tolerance has led to substantial research efforts to overcome this disadvantage by introducing reinforcements in the through-the-thickness direction, thereby reducing crack propagation and avoiding catastrophic failure by delamination. These 3D textile structures are produced by textile processes like weaving, braiding, stitching and knitting.

To the performance requirements of high damage tolerance, high specific stiffness and strength, reduced production cost is an increasingly important consideration. A lot of effort has been directed towards research for introducing mass production and

its associated reduced manufacturing cost. This is of great importance, if these materials are to be adopted by the automotive industry with their requirements of high volume production.

With these two objectives of mechanical performance (particularly through-the-thickness) and low cost production, 3D-woven textile composites have been shown to be promising candidates. 3D-weaving allows the production of near net shape structures as integral units directly from the loom (examples see Figure 1), thus avoiding the use of joints or fasteners.

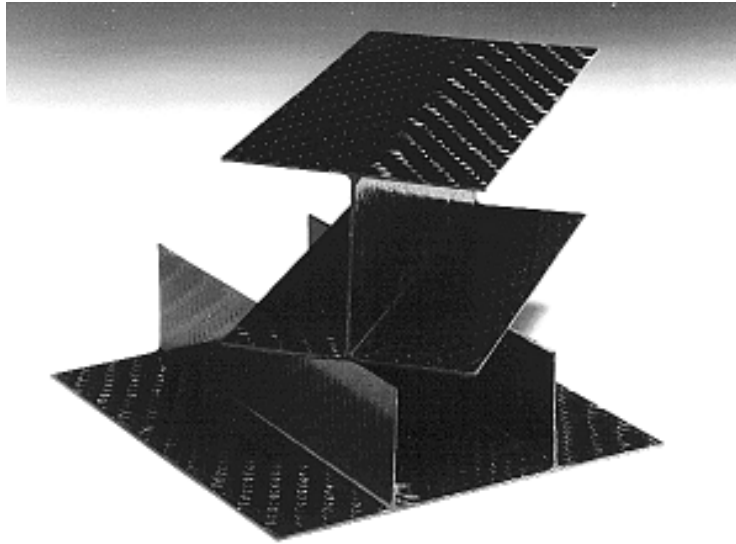


Figure 1: Integrally woven double-bladed T-skin and I-beam<sup>1</sup>

The benefits of 3D-weaving are twofold; firstly the improvement in damage tolerance by introducing through-the-thickness reinforcements and secondly by enabling the production of integrated near net shape structures, thus reducing the labour costs associated with the lay-up of laminates.

However, additional to the selection of the matrix material and the fibre type, a set of new design variables appeared in relation to the definition of the weave structure itself. Figure 2 shows some examples of complex 3D-weave structures developed by Soden at the Engineering Composites Research Centre. The through-the-thickness yarns can be clearly seen linking several layers together.

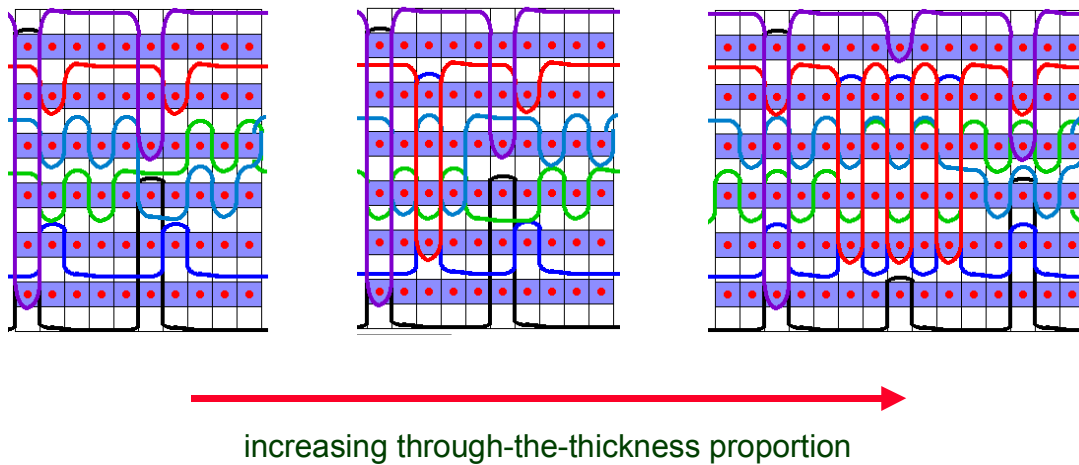


Figure 2: Examples of complex 3D-weave structures (cross-sections)<sup>2</sup>

The weaving process is described by Soden et al<sup>3</sup> as follows:

“The weaving of multilayer reinforcements has developed into a complete process, utilising modified weave structures and lift plans with through-the-thickness yarns incorporated as part of the weave design<sup>4</sup>. Multilayer woven reinforcements can be manufactured on conventional textile machinery with few mechanical modifications to produce reinforcements with fibres orientated in the warp (X), weft (Y), and through-the-thickness (Z) directions. Specific proportions of yarns can be arranged into each of three mutually perpendicular directions. For many fabrics produced on conventional looms, the warp yarns undertake a dual role. Firstly they create the (X) axis proportion, which is usually in the principal stress direction, and secondly they form the through-the-thickness or (Z) element. Thus for a given percentage of yarn in the (Y) direction, increasing the (Z) proportion results in an equivalent reduction in the (X) proportion, resulting in a loss of engineering properties in that direction. Such reinforcements demonstrate good delamination resistance when compared with laminated composites fabricated by the plied lay-up method<sup>13</sup>, in addition reproducibility of preforms is more readily achieved because the manual lay-up element is greatly reduced. [...]

The difficulty associated with weaving multilayer fabrics on conventional looms can increase if a multilayer shaped reinforcement is required. An approach is therefore taken where shaped reinforcements are produced on conventional looms by utilising the concept of initially weaving the shaped reinforcement in a flat multilayer form, and folding or opening to the desired shape after removal from the loom.”

## ***1.2 Application of textile composite materials***

Two examples of the application of 3D-woven carbon fibre textile composite materials investigated at the Engineering Composites Research Centre are a composite component of a lower leg prosthesis and a beam with T-shaped cross section. These are presented from the perspective of illustrating the need for structural analysis of such composite components. Due to the lack of a technique for structural analysis of components made of these advanced materials, the design methodology was very much based on an empirical approach. In the following sections the design methodology is described and areas for the possible application of structural analysis are highlighted. From these identified aspects of structural analysis, the requirements for an analysis system can be derived.

### ***1.2.1 Composite component of a lower leg prosthesis***

Within the Northern Ireland Bioengineering Centre (NIBEC) a prosthesis for a below knee amputee was developed. Lower-limb prostheses easily provide static structural supports, but not dynamic functions that correspond to muscle activities that have been lost. Therefore, good locomotion by the amputee requires a prosthesis, which shows the same dynamic behaviour as the lost limb.

The new approach in the design is to utilise a composite material instead of conventional engineering materials, such as steel, aluminium or titanium. The purpose of this new design approach is to achieve improvements in terms of

increased convenience for the patient. Therefore, the inherent advantages of fibre reinforced plastics were used, which are described briefly in the following paragraphs. The use of a composite material has two main advantages<sup>5</sup>:

- Lightweight

The total weight of the prosthesis is the most important consideration from the amputee's perspective. The remaining muscle mass in the residual limb defines an upper limit for the total weight of the prosthesis. Reduced weight leads to greater mobility and less fatigue for the amputee.

- Multifunctionality

A main advantage of fibre reinforced plastics is the capacity for part integration leading to a reduction in parts count. The same product configuration constructed in aluminium and titanium has, in the case of lower limb prosthesis, sometimes twice as many component parts.

The disadvantage of laminated composites is the low damage tolerance as described in section 1.1, which can be significantly reduced by using 3D-woven textile composites. The increase in impact strength is a very important consideration, because people using prostheses often lead an active lifestyle (see Figure 3), which involves activities like running, jumping or kicking. The impact load on a lower limb prosthesis can be significant.



Figure 3: An athlete with similar lower leg prostheses<sup>6,\*</sup>

The prosthesis consists of the following elements (see Figure 4):

- an adapter to fasten the prosthesis to the remaining part of the leg
- a connection between the fastening and the composite component
- the composite component
- the sole, also a composite
- a wedge shaped support between sole and composite component

The theme of the project with NIBEC was the analysis of the composite component. Its behaviour is essential for the quality of the complete prosthesis.

---

\* Aimee Mullins (USA), 200 m, Paralympics, Atlanta (USA), August 1996



Figure 4: Lower leg prosthesis developed at the University of Ulster

The below-knee amputee has lost part of their locomotive system not only in terms of the static supporting structure, but also in the dynamic function of the foot-ankle complex. The repeating element in the locomotion is the gait cycle. A complete gait cycle is defined as the time from which the heel of one foot contacts the ground to the next heel-contact of the same foot<sup>7</sup>. During the stance phase three characteristic moments occur (see Figure 5), which were chosen for the calculation. These are as follows:

- after heel-contact, when the maximum reaction force acts (1)
- at mid-stance, when the whole body weight takes place (2)
- before toe-off, at maximum push-off (3)

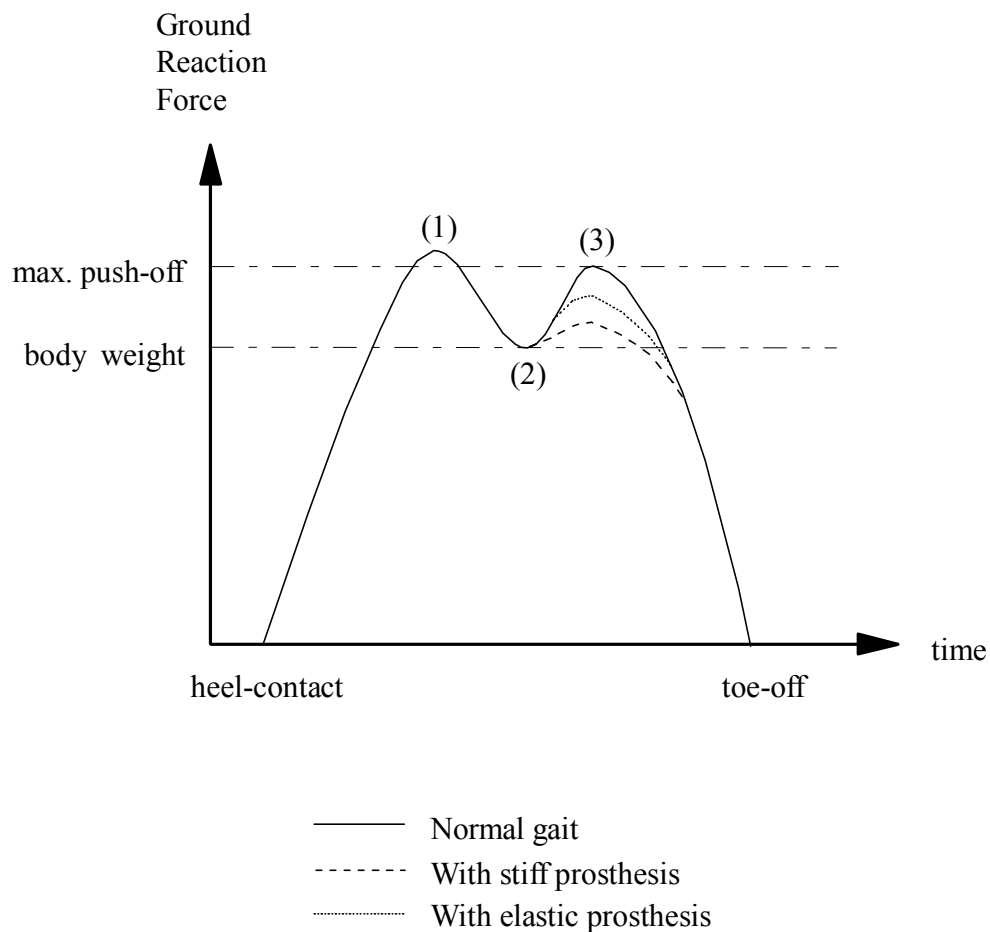


Figure 5: Forces during stance phase

In order to achieve a gait as close as possible to natural for the amputee, it is essential that a sufficient amount of deformational energy is stored in the prosthesis and released as kinetic energy during late-stance phase.

Furthermore the deflections of the prosthesis have to be within a certain range. If the subject using the prosthesis does not show the above described behaviour, the consequences would be that running, jumping and even walking are performed only with difficulty and at a high energy cost to the user<sup>8</sup>.

The above-described aspects impose the following design requirements:

- The proceedings during the swing-phase determine the amount of elastic energy to be stored in the composite component of the lower-leg prosthesis.

- Different forces act on the limb component during the stance phase. These forces are responsible for the deflections, which have to be within a certain range.

Two different designs were analysed. They were made of the same lay-up to provide the possibility to investigate the exclusive influence of the geometry of the composite component. The first, a J-shaped design, has been already tested in practical operation. Limitations, such as an insufficient amount of elastic energy storage, became evident. In the case of the improved second design, an attempt was made to overcome these problems. Firstly, by altering only the geometry of the component. A subsequent follow-up was then to involve local stiffness tailoring to achieve an even greater storage of elastic energy in the composite component.

The stiffness tailoring of the material was done by using I-DEAS to analyse the effects of changes of the lay-up of the laminate and subsequently using the optimised lay-up to translate this stiffness to a 3D-woven textile material. This approach was necessary, as there was no design tool available to cater for this new type of material. Additionally, it was not possible to predict any stress concentrations around holes used to connect the different parts of the prosthesis when using 3D-woven textile composites. This had to be done experimentally, or by observing the behaviour of the prosthesis while in use.

### *1.2.2 T-sections*

One of the main advantages of 3D-woven textile composites is the production of near net shape structures as integral units directly from the loom. This advantage of 3D-woven composites over laminated composites leads to substantially reduced labour content and the ease of handling compared to the manually intensive lay-up process for laminates. With the through-the-thickness reinforcement another disadvantage of laminates is minimised if not eliminated - the typical failure mode of delamination.

Table 1 shows a comparison for a T-shaped stiffener manufactured of steel and 3D-woven composites with respect to the weight of the parts with equal bending stiffness.

	steel	Composite (6 layer twill based 3D-woven fabric, carbon/epoxy)
bending stiffness $EI$ [Nm <sup>2</sup> ]	2400	2400
weight per unit length [ $\frac{\text{kg}}{\text{m}}$ ]	0.50	0.32
relative weight [%]	100	64

Table 1: Comparison of weights of parts with equal stiffness

A series of 6 layer 3D-woven T-sections and a laminated control sample were impregnated with an epoxy resin and cured at 150 °C in an autoclave at 12 bar pressure to form a range of shaped reinforced composites. The reinforcements for this application were designed specifically to overcome the problems of resin-rich areas found at the web/flange interface in 6-layer structures. Interplane strength tests, devised for this particular component type, were carried out in order to assess the reinforcement quality. The results indicate that the type and amount of interlinking influence the mode of failure but their relationship with interplane strength is complex.

This interplane strength test is, in principle, a tension test where a force is applied at both ends of the flange. The aim of this test is to determine the reinforcement (i.e. the weave structure) quality in the cleavage area (see Figure 6) at the web/flange interface, by measuring the initial failure load, the peak load and by recording the force/deflection curve. Test results are therefore only valid if failure occurs along the mid-plane of the reinforcement in the web.

This test was devised in order to assess the quality of a particular feature of the part, which is associated with the manufacturing technique. However there is also the need for other tests (e.g. bending or shear) approximating more closely to the in-service loading.

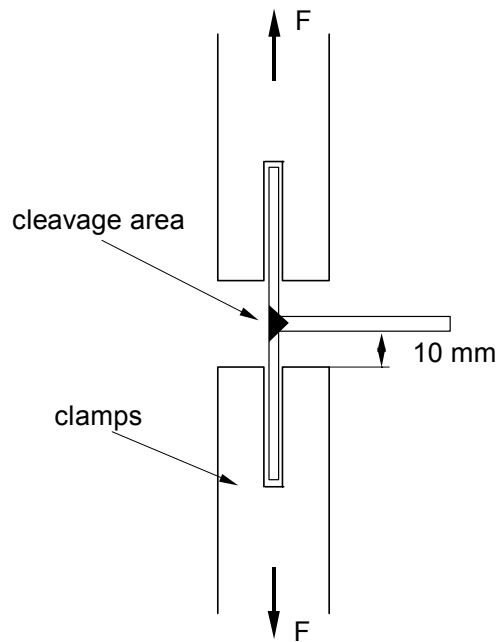


Figure 6: Test set-up for interplane testing

Test specimens with dimensions of (50 mm length)  $\times$  (50 mm width)  $\times$  (50 mm height) were prepared for interplane strength testing. The specimens were clamped over the entire width and were aligned carefully so that the web was horizontal, as illustrated in Figure 6. The loading speed was set relatively small to 1 mm/min, as this is a quasi-static test<sup>9</sup>. Research on the tensile testing of 3D textile composites has been undertaken by NASA<sup>10,11,12</sup>. Although this work was concerned with plaque type specimen, it gave a general indication of the levels of loading speed and specimen dimensions. Tensile testing of composite T-pieces manufactured with 3D-woven glass fibres was also conducted in the Engineering Composites Research Centre at the University of Ulster<sup>13,14</sup>.

Figure 7 illustrates a typical force/deflection curve for an interplane test. In this figure the initial failure load is the force when the first crack occurs and the peak load is the highest force reached after the first crack has been initiated.